Atmos. Chem. Phys., 14, 7941–7951, 2014
www.atmos-chem-phys.net/14/7941/2014/
doi:10.5194/acp-14-7941-2014

Atmospheric Chemistry and Physics
Open Access

Production and growth of new particles during two cruise campaigns in the marginal seas of China

X. H. Liu[1], Y. J. Zhu[1], M. Zheng[2], H. W. Gao[1], and X. H. Yao[1,3]

[1]Key Laboratory of Marine Environment and Ecology, Ministry of Education of China, Ocean University of China, Qingdao 266100, China
[2]State Key Joint Laboratory for Environmental Simulation and Pollution Control, College of Environmental Sciences and Engineering, Peking University, Beijing 100871, China
[3]Qingdao Collaborative Center of Marine Science and Technology, Qingdao 266100, China

Correspondence to: X. H. Yao (xhyao@ouc.edu.cn) and M. Zheng (mzheng@pku.edu.cn)

Received: 21 November 2013 – Published in Atmos. Chem. Phys. Discuss.: 28 January 2014
Revised: 12 May 2014 – Accepted: 8 June 2014 – Published: 11 August 2014

Abstract. In this paper, we investigated production and growth of new particles in the marine atmosphere during two cruise campaigns in China Seas using a Fast Mobility Particle Sizer. Only eight new particle formation (NPF) events (> 30 min) occurred on 5 days out of 31 sampling days, and the subsequent growth of new particles was observed only in five events. Apparent formation rates of new particles (in the range of 5.6–30 nm) varied from 0.3 to 15.2 particles $cm^{-3}\,s^{-1}$ in eight events, and growth rates ranged from 2.5 to 10 $nm\,h^{-1}$ in five NPF events. Modeling results simulated by US EPA Community Multi-scale Air Quality Model (CMAQ) showed that ammonium nitrate (NH_4NO_3) was newly formed in the atmosphere over the corresponding sea zone during 2 out of 5 events, in which new particles partially or mostly grew over 50 nm. However, in the remaining three events, new particles cannot grow over 30 nm, and the modeling results showed that no NH_4NO_3 was newly formed in the corresponding marine atmosphere. Modeling results also showed that formation of secondary organics occurred through all new particle growth periods. Difference between the two types of new particle growth patterns suggested that a combination of ammonium nitrate and organics newly formed likely contributed to the growth of new particles from 30 nm to larger size. However, the findings were obtained from the limited data, and the simulations of CMAQ also suffered from several weaknesses such as only having three size bins for different particles, lack of marine aerosol precursors, etc. More future studies are thereby needed for confirmation.

1 Introduction

Atmospheric particles play important roles in regional visibility deterioration and global climate change by directly scattering and absorbing the sunlight and indirectly acting as cloud condensation nuclei (CCN) (Sloane et al., 1991; Curtius, 2006; IPCC, 2007; Luo and Yu, 2011), and they have primary and secondary origins (Holmes, 2007; Kulmala and Kerminen, 2008; Pierce et al., 2012; Riipinen et al., 2011, 2012; Yao and Zhang, 2011). Nucleation has been reported as an important secondary source of atmospheric particles because it can quickly increase the number concentration of atmospheric particles from hundreds to dozens of thousands particles per cubic centimeter air in a few hours (Kulmala and Kerminen, 2008). However, atmospheric particles < 30 nm in diameter are conventionally considered to be nucleation mode particles, and particles in this size range are less likely to be activated as CCN under the typical range of atmospheric supersaturation (Dall'Osto et al., 2005; Dusek et al., 2006; Quinn et al., 2008). New particles growing over 50 nm in diameter have been found to be an important source of CCN while ∼ 80 nm particles can be activated to be CCN at a moderate supersaturation (e.g., ∼ 0.2 %; Petters and Kreidenweis, 2007; Pierce and Adams, 2009; Pierce et al., 2012; Riipinen et al., 2011, 2012). The size of new particles can be used to roughly evaluate their potential as CCN, although other factors such as their chemical composition and mixing state also affect the potential (Dusek et al., 2006; Quinn et al., 2008; Kerminen et al., 2012). However, it is still quite unclear

which chemicals contribute to the condensational growth of new particles to CCN size (Kulmala et al., 2013), particularly the growth of new particles from ∼ 30 nm to CCN size.

Oceans account for approximately 70 % of areas on the earth. Huge efforts have been taken to improve understanding of the relationship between production of new particles in marine atmosphere and their impacts on the climate in the last 3 decades (Charlson et al., 1987; O'Dowd et al., 2007; Quinn and Bates, 2011). Several earlier studies focused on new particle formation (NPF) in remote marine atmosphere and some clear coastal environments such as Mace Head, where dimethylsulfide (DMS) and iodine have been proposed to be important precursors for new particles (Cover et al., 1996; Clarke et al, 1998; O'Dowd et al., 2002; O'Dowd et al., 2007; Chang et al., 2011). In polluted marine atmosphere, high concentrations of secondary particulate species generated from anthropogenic and/or biogenic precursors as well as a small amount of particulate methanesulfonic acid from marine biogenic sources were frequently observed, and these observed species were proposed to have important impacts on regional climate (Yang et al., 2009; Shi et al., 2010; Feng et al., 2012; Wang et al., 2014). For indirect climate effects, the number concentration of atmospheric particles is critical. However, direct measurements of NPF events are still limited, and the same can be said for assessing their potential contribution to CCN (Lin et al., 2007). In addition, the characters of NPF among in polluted, remote marine and clear coastal environments could be very different. Thus, more observations for NPF events in polluted marine atmosphere are essential.

To improve understanding the characters of NPF events in polluted marine atmosphere in different extents and evaluating their potential climatic impacts, we investigated NPF and their subsequent growth in the marginal seas of China including the Yellow Sea and the East China Sea during two cruise campaigns from 16 October to 5 November 2011 and from 2 to 11 November 2012. A Fast Mobility Particle Sizer Spectrometer (FMPS) was used for on-board sampling to study NPF events, and the US EPA Community Multi-scale Air Quality Model (CMAQ) was used to simulate chemical and physical processes of particulate species over the study marginal seas to facilitate data analysis. On 5 days during the two campaigns, eight NPF events with or without a subsequent growth of new particles were observed. An in-depth analysis was conducted to interpret these events with particular attention to investigate factors determining the growth of 30–40 nm new particles to larger size.

2 Experimental

2.1 Cruise routes, particle sizers and computer method

In the fall of 2011 and 2012, two cruise campaigns were organized by Ocean University of China (OUC) using a research vessel *Dongfanghong 2* (Fig. 1a and b). The two campaigns were to provide services for research projects funded by National Natural Science Foundation of China, and these projects covered a variety of basic research from seabed to lower layer marine atmosphere. The cruise route during the period 16 October to 5 November 2011 included the south Yellow Sea and the East China Sea, while the second campaign was limited in the south Yellow Sea during the period of 2–11 November 2012.

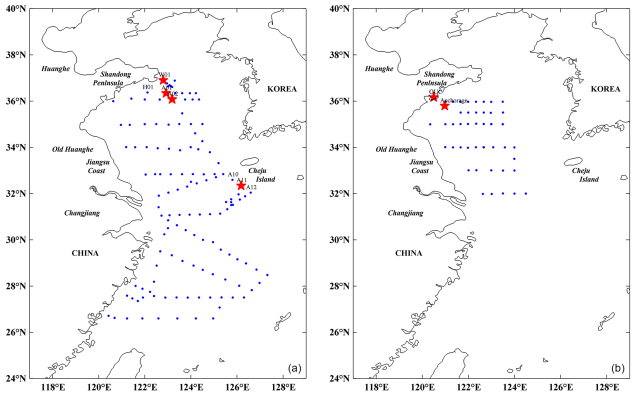

Figure 1. Cruise track during China Sea **(a)** cruise during 16 October–5 November in 2011 and **(b)** cruise during 2–11 November in 2012. Pentacles represent the locations of particle burst events.

A FMPS (TSI Model 3091) downstream of a dryer (TSI, 3091) was used for measuring number concentrations of marine atmospheric particles in 1-second time resolution, which was placed on the front board of *Dongfanghong 2*. To investigate the potential relationship of NPF events between inland and marine atmosphere, simultaneous measurements were conducted on the top floor of a five-story building on the campus of Ocean University of China (lat: 36.1° N, long: 120.5° E; distance to the nearest coast line is 7.5 km) using a NanoScan Scanning Mobility Particle Sizer Spectrometer (SMPS) nanoparticle sizer (TSI, 3910) in November 2012, but not in November 2011. The sizer was equipped with a Radial Differential Mobility Analyzer (RDMA) and an internal Condensation Particle Counter (CPC) and operated in 1-minute time resolution. Particle apparent formation rate (J_{30}) was calculated using the method provided by Dal Maso et al. (2005):

$$J_{30} = \mathrm{d}N_{<30\,\mathrm{nm}}/\mathrm{d}t + F_{\mathrm{growth}} + F_{\mathrm{coag}}, \quad (1)$$

where $N_{<30\,\mathrm{nm}}$ is the number concentrations of the 5.6–30 nm particles for the FMPS and 10–30 nm for the NanoScan SMPS during the initial 1–2 h of new particle burst; F_{growth} (the flux of particles grow out of the size range; we chose the size range for the nucleated particles to be 5.6–30 nm) is conventionally assumed to be zero, because particles rarely grew out of 30 nm in the initial 1–2 h (Dal Maso et al., 2005); and F_{coag} is the sum of particle–particle inter- and

heterocoagulation rate calculated in the same way as Yao et al. (2005).

Particle size distributions in this study were not unimodal most of the time, and they were dominated by bimodal distribution. Therefore, aerosol particle size distributions in this study are fitted with the multi-lognormal distribution function (Whitby, 1978), which is expressed mathematically by

$$f(D_{\mathrm{p}}, D_{\mathrm{pg},i}, C_i, \sigma_{\mathrm{g},i}) = \sum_{i=1}^{n} \frac{C_i}{(2\pi)^{1/2}\log(\sigma_{\mathrm{g},i})} \times \exp\left[-\frac{[\log(D_{\mathrm{p}}) - \log(D_{\mathrm{pg},i})]^2}{2\log^2(\sigma_{\mathrm{g},i})}\right], \quad (2)$$

where D_{p} is the diameter of aerosol particle. Three parameters characterize an individual lognormal mode i: the mode number concentration C_i, geometric variance $\sigma^2_{\mathrm{g},i}$, and geometric mean diameter $D_{\mathrm{pg},i}$. The number of individual lognormal modes that characterize the particle number size distribution is denoted by n (i is in the range of $1-n$). In this study, n is usually equal to 2, and $D_{\mathrm{pg},1}$ represents the geometric median diameter of new particles followed by particle growth in the observed events. The growth of preexisting Aitken mode particles was also observed in this study, and $D_{pg,2}$ represents the geometric median diameter of the preexisting particles.

Particle apparent growth rate (GR) in this study was calculated by

$$\mathrm{GR} = \frac{\Delta D_{\mathrm{pg},i}}{\Delta t}, \quad (3)$$

where Δt is the time slot for the growth of particles. Particle apparent shrinkage rate (SR) was calculated using the same equation as GR, but the value is negative.

2.2 Model description

The US EPA Community Multi-scale Air Quality Model (CMAQ v4.7.1; Byun and Ching, 1999) was used for simulating concentrations of gases and particulate species in $PM_{2.5}$ during NPF events. The meteorological data were provided by the Weather Research and Forecasting (WRF) model (v3.2) (Skamarock et al., 2008) and processed by the Meteorological-Chemical Interface Processor (MCIP v3.3) for CMAQ-ready inputs. Emissions were generated on the basis of the NASA's project emission inventory (The Intercontinental Chemical Transport Experiment Phase B, INTEX-B; Q. Zhang et al., 2009; Liu et al., 2010a), which included major air pollutants such as SO_2, NO_x, CO, and 30 lumped volatile organic compound species. The vertical resolution includes 14 logarithmic structure layers from the surface to the tropopause, with the first model layer height of 36 m above the ground level, while the horizontal resolution is 36 km × 36 km. Particle in CMAQ is represented by three lognormal subdistributions, i.e., Aitken, accumulation and coarse mode. Riipinen et al. (2011) and Ehn et al. (2014) recently reported the important role of extremely low volatility secondary organic aerosol (SOA) in growing < 30 nm new particles in continental atmosphere. In CMAQ version 4.7.1, four types of non-volatile SOA were simulated, while other SOA species was treated as semi-volatile (Carlton et al., 2010). Validation of CMAQ application in China has been reported by Liu et al. (2010a, b). The CMAQ model does not include chemical reactions of amines which have been proposed as an important species to grow nucleated particles (Smith and Mueller, 2010; Riipinen et al., 2012; Zhang et al., 2012; Kulmala et al., 2013). Thus, contributions of amines to new particle growth will not be discussed in this study.

2.3 On-site meteorological data and satellite data

Wind speed, wind direction, relatively humidity, air temperature and solar radiation were measured continuously on board and synchronously. Daily averaged sea surface chlorophyll *a* concentrations were derived from Standard Mapped Image products observed by Moderate Resolution Imaging Spectroradiometer (MODIS)/AQUA SMI products. Horizontal resolution is 4 km × 4 km (Tan et al., 2011).

3 Results

NPF events (> 30 min) were observed on 4 days during the cruise campaign in 2011. However, there was only 1 day when NPF events were observed in the cruise campaign in 2012 (Supplement Fig. S1a and b). On the same day, a NPF event was also observed at the site of OUC. All these NPF events in the marine atmosphere started to be observed at the locations, which are 30–120 km away from the nearest coastline (Fig. 1a and b, Table 1). In these events, the total number concentration of < 30 nm particles increased from $\sim 0.5 \times 10^3$ particles cm^{-3} to $\sim 2.5 \times 10^4$ particles cm^{-3} within 0.5–4 h. We will first examine the production and growth processes of the events in 2012 in Sect. 3.1, while in Sects. 3.2 and 3.3 events in 2011 will be studied.

3.1 NPF events in the fall cruise campaign of 2012

In November 2012, two particle sizers were used for measurements on board and on the land, respectively. The observation can allow an investigation of regional characteristics of NPF events. A heavy rain event occurred at night on 3 November 2012 with wind speed of 10–14 $\mathrm{m\,s}^{-1}$. The rainfall and the strong wind substantially removed preexisting atmospheric particles, and NPF events were observed both in the marine and coastal atmosphere in the daytime of 4 November (Day 1, Fig. 2). On Day 1, *Dongfanghong 2* was anchored at approximately 80 km distance southeast of OUC, and the location was about 60 km away from the nearest coastline (Fig. 1b).

Table 1. Major characteristics of NPF events over marginal seas of China in the fall of 2011 and 2012.

Day	No.	Period	J_{30} (particles cm^{-3} s^{-1})	GR ($nm\,h^{-1}$)	Location
Day 1 4 November 2012	2	7:50–8:43 9:24–18:35	1.4 3.1	– 5.0 (first stage, 6–39 nm) 10.0 (second stage, 34–47 nm)	∼ 60 km from the land
Day 2 17 October 2011	2	10:00–10:30 10:30 (17 October)– 03:50 (18 October)	15.2 4.1	– 2.5 (first stage, 6–42 nm) 7.5 (second stage, 42–55 nm)	H01-W01, ∼ 30 km from the land
Day 3 18 October 2011	1	10:15–18:20	7.5	3.5 (6–28 nm)	∼ A01, 80 km from the land
Day 4 19 October 2011	2	10:00–11:13 11:13–18:30	0.3 1.1	3.4 (6–22 nm)	A02, 120 km from the land
Day 5 26 October 2011	1	10:30–15:30	1.6	4.4 (6–21 nm) −3.5 (Shrinkage, 21–17 nm) 16.7 (58–83 nm)*	A10–A12, 110 km from the land

Note: * is the growth rate of preexisting Aitken mode particles.

3.1.1 Formation rates of new particles

Two NPF events were observed on Day 1 in the marine atmosphere. The first one had been observed since 07:50 LT and reached the maximum at 08:43 LT (Fig. 2a and b). The initial size of new particles was ∼ 6 nm, which is the detection limit of FMPS. The nucleation mode particles (< 30 nm) increased from $< 1.0 \times 10^3$ particles cm^{-3} before 07:50 to 1.0×10^4 particles cm^{-3} at 08:43 LT, and the apparent formation rate of new particles was calculated to be 1.4 particles $cm^{-3}\,s^{-1}$. No particle growth was observed before 08:43 LT. The second NPF event was observed after 09:24 LT. Nucleation mode particles increased from 0.4×10^4 to 2.5×10^4 particles cm^{-3} with the apparent formation rate of 3.1 particles $cm^{-3}\,s^{-1}$ during the period of 09:24–10:32 LT. The formation rates of two events are all within the range of typical new particle formation rates in the atmosphere (0.01–10 particles $cm^{-3}\,s^{-1}$; Kulmala and Kerminen, 2008).

On Day 1, a NPF event was also observed at OUC where the measurement was made during the period 09:30 to 15:13 LT (Fig. 2d and e, we stopped the sampling after 15:13 LT because of high relative humidity). The new particle growth curves show that the curve in the Yellow Sea after 09:30 LT almost parallels that at OUC (Supplement Fig. S2a), and the event observed at OUC advanced 1–1.5 h relative to the event observed in the Yellow Sea. Also, $N_{<30\,nm}$ values at the higher concentration zones – e.g., $1.6 \pm 0.3 \times 10^4$ particles cm^{-3} during 10:50 to 12:30 LT in the Yellow Sea and $1.6 \pm 0.1 \times 10^4$ particles cm^{-3} during 10:50 to 13:00 LT at OUC (upplement Fig. S2b) – were comparable. These suggested that NPF events occurred regionally on Day 1, but the start times were location-dependent. These higher $N_{<30\,nm}$ values at OUC varied in a narrow range, suggesting spatial homogeneity of nucleation in the rural area. However, these values in the Yellow Sea varied a lot. This could be due to a spatial heterogeneity of nucleation in the marine atmosphere or other unknown factors.

3.1.2 Growth rates of new particles

A two-phase new particle growth was observed in the Yellow Sea on Day 1 (Fig. 2b); 09:24–15:45 LT was the first-phase growth period while the second-phase growth occurred during 17:25–18:35 LT. During the first-phase growth period, the calculated $D_{pg,1}$ of new particles increased up to 39 nm with the growth rate of 5.0 nm h^{-1} (Fig. 2b, Table 1), which is close to the growth rate of 5.5 $nm\,h^{-1}$ at OUC. It is interesting that no growth was observed between 15:45 and 17:25 LT in the Yellow Sea, but a slight decrease of the $D_{pg,1}$ was observed from 39 nm at 16:44 to 34 nm at 17:25 LT. The decrease could be explained by the shrinkage of new particles (Yao et al., 2010; Young et al., 2013). However, it also could be due to the change in measured air mass. At OUC, the $D_{pg,1}$ did not increase after 14:20 LT and fluctuated at 35 ± 1.3 nm between 14:20 and 15:13 LT (Fig. 2e). The observations suggested that ∼ 40 nm was likely a bottleneck for the growth of new particles in the daytime on Day 1, although the reasons remain unknown.

The $D_{pg,1}$ in the marine atmosphere restarted to increase from 34 nm at 17:25 to 47 nm at 18:35 LT (after this, sampling was stopped due to high relative humidity), suggesting that the bottleneck of ∼ 40 nm was broken up. The growth

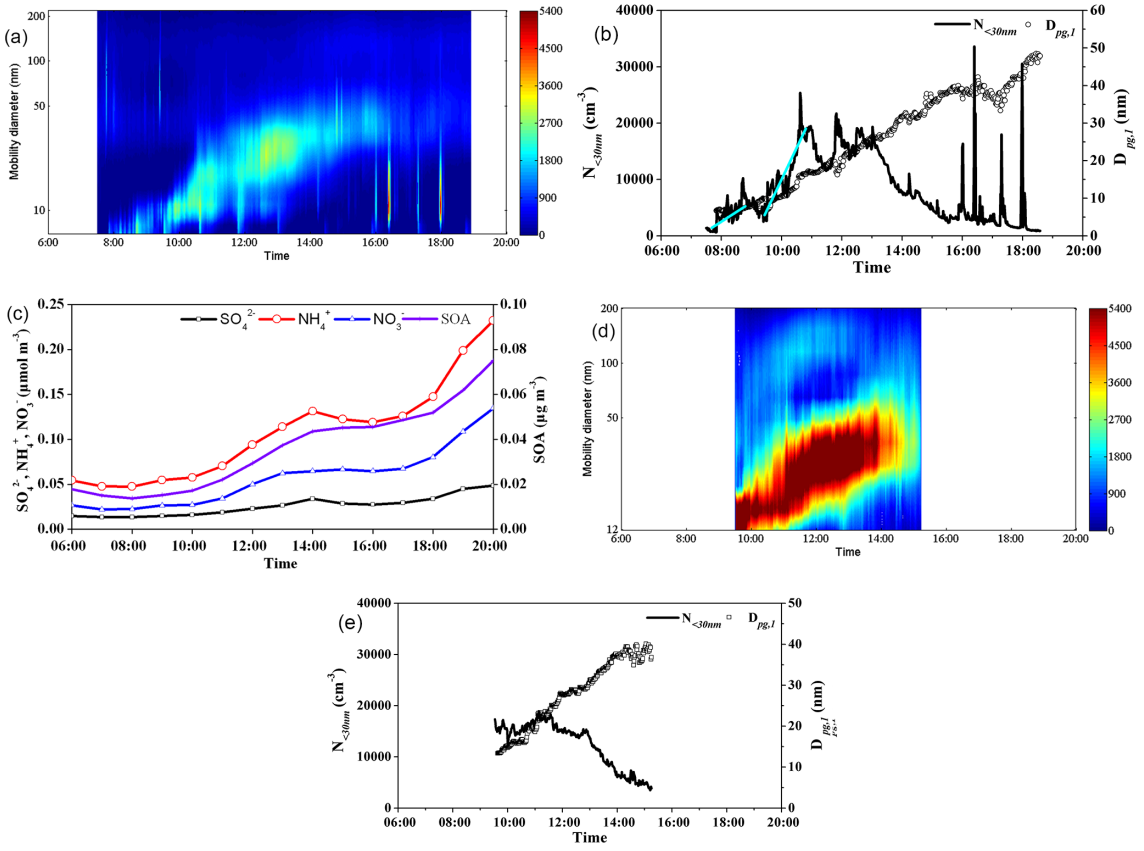

Figure 2. New particle formation events in marine **(a–c)** and coastal atmosphere on 4 November 2012 **(d–e)**, **(a)** particle number concentrations from FMPS (cm^{-3}), **(b, e)** variations of median diameter of particle mode ($D_{pg,1}$) and number concentrations of nucleation mode particles ($N_{<30\,nm}$) in marine and coastal atmosphere, **(c)** CMAQ simulation of SO_4^{2-}, NH_4^+, NO_3^- and SOA in $PM_{2.5}$ in marine atmosphere, **(d)** particle number concentrations from SMPS (cm^{-3}).

was referred to as the second-phase growth. The second-phase growth rate was calculated to be 10 nm h^{-1}, and the value was almost twice that of the first-phase growth rate. At OUC, we did not observe the second-phase growth on Day 1 because we stopped sampling after 15:13 LT. Ehn et al. (2010) reported four NPF events over the Irish west coast with the averaged growth rate of ~ 3 nm h^{-1}. In remote marine atmosphere, growth rates of nucleated particles were reported to be in the range of 0.1–1 nm h^{-1} (Kulmala and Kerminen, 2008; O'Dowd et al., 2010). The obviously larger growth rates observed in this event than other studies could be related to continental outflow of air pollutants, which will be discussed later.

When the volume concentration of particles is considered, the amount of chemical species required for the new particle growth during the second-phase growth period (17:25–18:35 LT) was almost the same as that during the entire first-phase growth period (09:24–15:45 LT). This indicated that much stronger gas-particle condensation processes occurred after 17:25 LT (second-phase growth), when the solar radiation substantially decreased down to a low value. Photochemical reactions were expected to be very weak at that period and cannot explain the sudden and strong condensation during the second-phase growth. Alternatively, it was more likely associated with processes by thermodynamic equilibriums. For example, when the product of nitric acid (HNO_3) and ammonia (NH_3) gaseous concentrations were higher than the thermodynamic equilibrium constant of NH_4NO_3, formation of NH_4NO_3 can suddenly take place. Formation of NH_4NO_3 often occurs in the evening or night because of decreasing ambient temperature and increasing relative humidity.

3.2 Strong NPF events in the fall cruise campaign of 2011

Two NPF events were also observed on 17 October 2011 (Day 2) in the marine atmosphere. A strong short-term NPF event was observed between 10:00 and 10:30 LT, and the estimated formation rate was 15.2 particles cm^{-3} s^{-1} (Fig. 3a and b). No subsequent growth of new particles was observed during the short-term event. A longer NPF event was

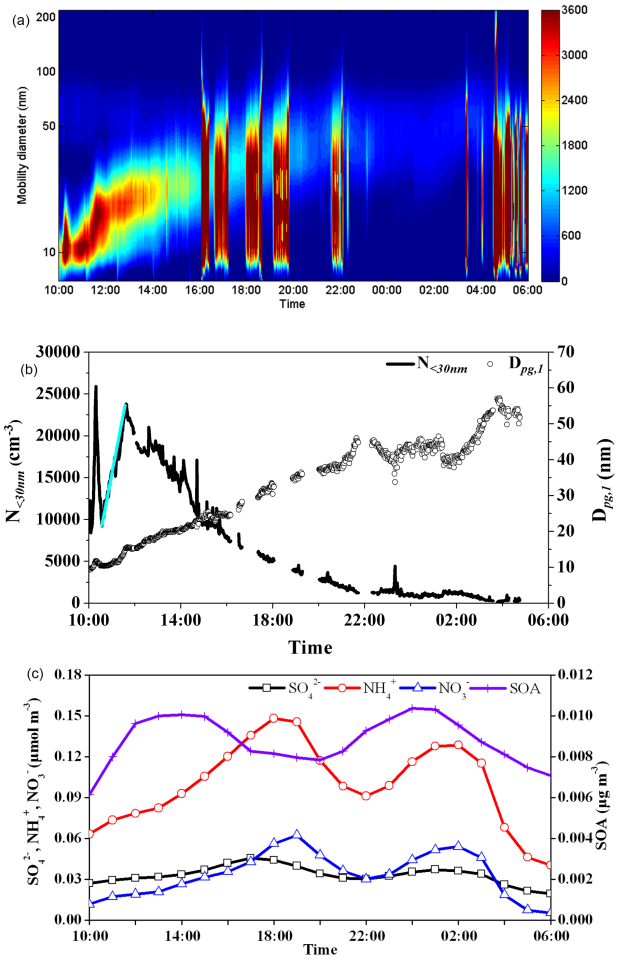

Figure 3. New particle formation on 17 October 2011 (**a** particle number concentrations from FMPS (cm^{-3}), **b** variations of median diameter of particle mode ($D_{pg,1}$) and number concentrations of nucleation mode particles ($N_{<30\,nm}$), **(c)** CMAQ simulation of SO_4^{2-}, NH_4^+, NO_3^- and SOA in $PM_{2.5}$).

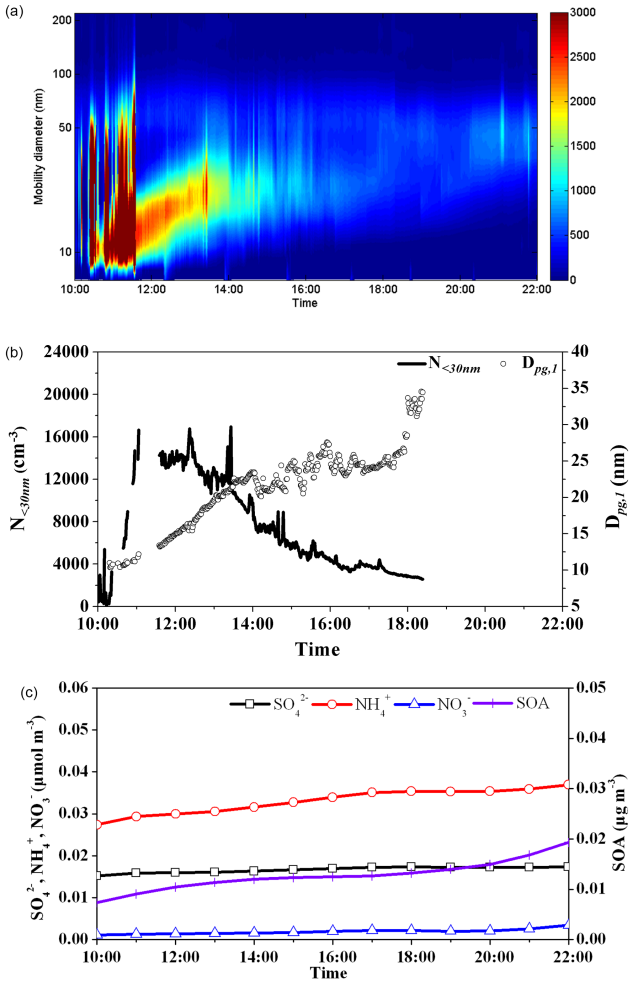

Figure 4. New particle formation on 18 October 2011, **a** particle number concentrations from FMPS (cm^{-3}), **(b)** variations of median diameter of particle mode ($D_{pg,1}$) and number concentrations of nucleation mode particles ($N_{<30\,nm}$), **(c)** CMAQ simulation of SO_4^{2-}, NH_4^+, NO_3^- and SOA in $PM_{2.5}$.

observed from 10:30 on Day 2 to 03:50 LT on 18 October 2011 (Day 3) when the ship sailed from H01 towards W01 (Fig. 1a). The ship was ∼ 30 km from the coastline of Shandong Peninsula in China when the longer event started to be observed. The estimated formation rate in this longer NPF event was 4.1 particles cm^{-3} s^{-1} during the period 10:30 to 11:35 LT. The new particle growth rate was 2.5 nm h^{-1} during the period 10:30 to 21:40 LT on Day 2 (the first-phase growth). From 21:40 on Day 2 to 02:00 LT on Day 3, no particle growth was observed, and the $D_{pg,1}$ fluctuated at 42 ± 2 nm, which was similar to the particle growth bottleneck on Day 1. The second-phase particle growth occurred during the period 02:00 to 03:50 LT on Day 3 when the $D_{pg,1}$ increased from 42 nm to 55 nm with the growth rate of 7.5 nm h^{-1}. Again, strong gas-particle condensation processes likely occurred after 02:00 LT on Day 3 and broke up the bottleneck of ∼ 40 nm.

Only one NPF event was observed during the period 10:15–18:20 LT on Day 3 when the ship was situated ∼ 80 km away from the nearest coastline of Shandong Peninsula and sailed westbound towards A01 station in the Yellow Sea (Figs. 1a, 4a and b). However, hundreds of spikes associated with ship emissions occurred in the initial 1 h of the NPF event. When the signal of ship plumes was deducted (Supplement Fig. S3a and b, see supporting information for the approach), the estimated formation rate of new particles was 7.5 particles cm^{-3} s^{-1}. The growth rate was estimated to be 3.5 nm h^{-1} during the period 10:20 to 13:30 LT and decreased down to 1.2 nm h^{-1} between 13:30 and 18:20 LT. However, the maximum $D_{pg,1}$ was less than 30 nm before the signal of new particles disappeared (Table 1). The maximum

value was substantially lower than the size required to activate as CCN (Dusek et al., 2006; Petters and Kreidenweis, 2007; Quinn et al., 2008; Pierce and Adams, 2009).

3.3 Weak NPF events in the fall cruise campaign of 2011

Two weak NPF events were observed on 19 October 2011 (Day 4, Fig. 5a and b). A short-term NPF event started from 10:00 to 11:13 LT with the formation rate of 0.3 particles $cm^{-3}\,s^{-1}$ (Table 1). No obvious growth of new particles was observed. Similarly to Day 1 and Day 2, a longer NPF event was observed during 11:13–18:30 LT when the ship was anchored at A02 station (Fig. 1a). The station was ~ 120 km away from the nearest coastline. The estimated formation rate was 1.1 particles $cm^{-3}\,s^{-1}$. The rate was lower than the rates observed on Day 1–3. After 11:13 LT, the growth rate of new particles was estimated to be $3.4\,nm\,h^{-1}$. Again, the maximum $D_{pg,1}$ was less than 30 nm (Table 1). Note that a few periodic spikes of < 10 nm particles constantly occurred every 1 h and 40 min on that day, which were due to the sampling artifact. Based on 2-week side-by-side comparison between two identical FMPS in our previous studies (unpublished), we found that the sampling artifact was associated with high relative humidity, but it had negligible influence on the measurement of > 10 nm particles.

Only one NPF event was observed during the period 10:30 to 15:30 LT on 26 October 2011 (Day 5, Fig. 6a and b) when the ship sailed from A10 towards A12. The location was ~ 110 km away from Cheju Island of the South Korea (Fig. 1a). The estimated formation rate was 1.6 particles $cm^{-3}\,s^{-1}$, and the growth rate was $4.4\,nm\,h^{-1}$ in the initial 3 h. The $D_{pg,1}$ arrived at the maximum value of 21 nm at 13:30 LT and then apparently shrank down to 17 nm with a shrinkage rate of $3.5\,nm\,h^{-1}$. The shrinkage of new particles has been reported in coastal environments in daytime when photochemical reactions started to weaken (Yao et al., 2010; Young et al., 2013). This phenomenon could also be related to slight changes of measured air mass, but the influence should be minor. Since the time resolution of FMPS was as high as 1 s, rapid responses of $D_{pg,1}$ and $N_{<30\,nm}$ corresponding to slight changes of air mass can be detected. For example, $D_{pg,1}$ and $N_{<30\,nm}$ fluctuated dramatically during 14:00–17:00 LT on 18 October 2011 (Fig. 4). However, the $D_{pg,1}$ and $N_{<30\,nm}$ after 13:30 LT on Day 5 decreased smoothly for one and half hours. It is interesting that preexisting particles started to grow after 12:50 LT, with the $D_{pg,2}$ increased from 58 nm at 12:50 to 83 nm at 14:20 LT, and then fluctuated at 80 ± 2 nm (Supplement Fig. S4). The on-site recorded relative humidity varied from 62 % at 11:40 to 65 % at 14:40 LT and hygroscopic growth of particles cannot explain the growth factor of 1.3.

4 Discussion

4.1 Cause analysis of new particle formation

On Day 1, the apparent formation rate of new particles is 1.4 particles $cm^{-3}\,s^{-1}$ of the first short event, while the rate increased up to 3.1 particles $cm^{-3}\,s^{-1}$ in the second event. The ship was anchored at ~ 60 km distance from the coastline. Under the strong westerly wind ($10–14\,m\,s^{-1}$), it took approximately 1–2 h for air pollutants to be transported from the continent to the sea zone. Moreover, the growth curve of new particles in the Yellow Sea after 09:30 LT almost parallelled the growth curve at OUC, except for the 1–1.5 h delay (Supplement Fig. S2a). Thus, we postulated that the NPF event observed in the Yellow Sea after 09:24 LT was probably associated with air pollutants being transported from the continent. The modeling results in the sea zone, where the NPF event was observed, also showed that the continental outflow of air pollutants led to a slight increase of NH_4^+ and NO_3^- in concentrations after 08:00 LT (Fig. 2c and Supplement Fig. S5a). The modeling results apparently supported our postulation. However, we cannot exclude other possibilities because we have no measurement for those gaseous precursors of new particles.

The weaker NPF event between 07:50 and 08:43 LT might be associated with air pollutants being transported from the continent. However, it could also be related to ocean-derived biogenic precursors. The short duration suggested that it occurred only in the marine atmosphere. Moreover, the high wind speed would enhance air–sea exchange of gases and might increase ocean-derived biogenic precursors of new particles in concentrations, theoretically.

On Day 5, the NPF event occurred ~ 110 km away from the coastline of South Korea. Considering that the location of this event is far away from the polluted atmosphere, it can be speculated that it might be associated with ocean-derived gases. However, the satellite data showed that the concentration of chlorophyll *a* was less than $0.2\,mg\,m^{-3}$ in the sea zone (Supplement Fig. S6), which was much lower than the chlorophyll *a* concentration ($2–3\,mg\,m^{-3}$; Tan et al., 2011) in the presence of biogenic bloom in the East China Sea. Under that very low chlorophyll *a* condition on Day 5, ocean-derived biogenic precursors were unlikely important to this NPF event and other precursors were probably more important. The modeling results in the corresponding sea zone showed a slight increase of SO_4^{2-} and NH_4^+ in concentrations after 10:00 LT (Fig. 6 and Supplement Fig. S5e). The CMAQ indeed includes sea salt emissions, but there is no marine-derived gaseous sulfur, nitrogen, and carbon containing compounds. Thus, the NPF event was also possibly associated with the photochemical reactions of air pollutants being transported from the continent. Unlike on Day 5, NPF events on Day 2 were observed in the coastal sea (with ~ 30 km from the coastline). It is well known that chlorophyll *a* data suffer from a large interference of suspended

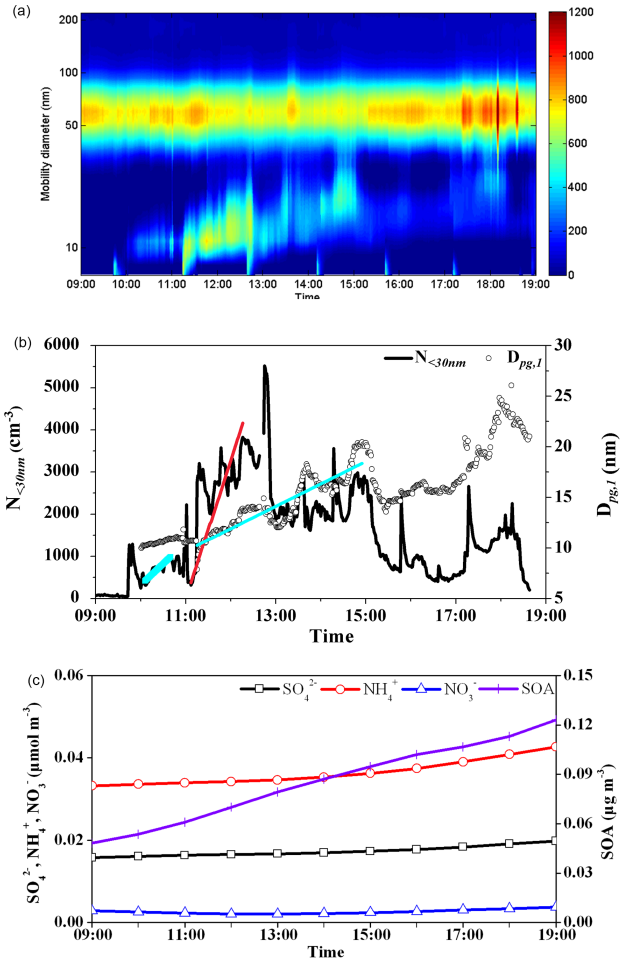

Figure 5. New particle formation on 19 October 2011 **a** particle number concentrations from FMPS (cm^{-3}), **(b)** variations of median diameter of particle mode ($D_{pg,1}$) and number concentrations of nucleation mode particles ($N_{<30nm}$), **(c)** CMAQ simulation of SO_4^{2-}, NH_4^+, NO_3^- and SOA in $PM_{2.5}$.

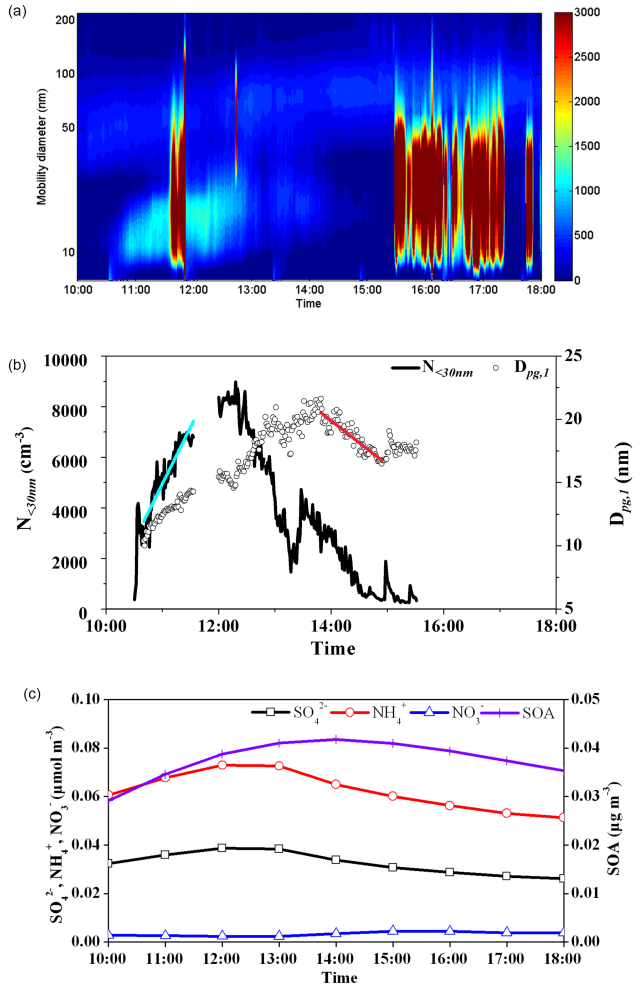

Figure 6. New particle formation on 26 October 2011 **a** particle number concentrations from FMPS (cm^{-3}), **(b)** variations of median diameter of particle mode ($D_{pg,1}$) and number concentrations of nucleation mode particles ($N_{<30nm}$), **(c)** CMAQ simulation of SO_4^{2-}, NH_4^+, NO_3^- and SOA in $PM_{2.5}$.

matters in coastal seawater which could not allow correctly justifying the potential influence of ocean biogenic precursors on this event (Chen et al., 2013). However, higher formation rates of new particles (e.g., 15.2 particles cm^{-3} s^{-1} between 10:00 and 10:30 LT and 4.1 particles cm^{-3} s^{-1} after 10:30) were observed on Day 2. The modeling results in the sea zone, where the NPF event was observed, showed that the continental outflow of air pollutants led to a simultaneous increase of SOA, NH_4^+ and NO_3^- in concentration after 10:00 LT (Fig. 3c and Supplement Figs. S5b and S7b). Thus, photochemical reactions of air pollutants from the continent possibly caused the NPF event on Day 2 after 10:00 LT.

We combined all observational data and modeling results to interpret NPF events on Day 3 and Day 4. The combining results still cannot allow identifying whether air pollutants transported from the continent or ocean-derived biogenic precursors caused those NPF events.

4.2 Cause analysis of new particle growth

Organics, ammonium sulfate and ammonium nitrate consisted of major parts of atmospheric particles in submicron size (O'Dowd and Leeuw, 2007; Smith et al., 2008; R. Zhang et al., 2009; Paasonen et al., 2010; Yao and Zhang, 2011; Ahlm et al., 2012). Ambient sulfuric acid gas (H_2SO_4) has been reported to yield a negligible contribution to condensational growth of > 10 nm new particles (e.g., 2 % of the GR of 7–20 nm particles; Riipinen et al., 2011; Ahlm et al., 2012; Pierce et al., 2012). This could be also true in the marine atmosphere of the marginal seas of China where the modeling mixing ratios of H_2SO_4 were less than 2 ppt during all NPF events (figures not shown). Organics were proposed to be important contributors to grow new particles to CCN (Riipinen et al., 2011; Pierce et al., 2012). On Day 3, 4 and 5, the

modeling results showed that SOA (see supporting information for detailed information of SOA modeling) was formed during the NPF events, suggesting that SOA could be an important contributor to grow new particles. The modeling results also showed that no NH_4NO_3 was formed during the entire new particle growth period on the 3 days in the marine atmosphere.

In addition, the temporal trend of the modeled SOA on Day 5 appeared to fit the new particle growth and subsequent shrinkage curve very well. The shrinkage of new particles occurred with a decrease of SOA in mass concentration (Fig. 6c and and Supplement Fig. S7e), but the preexisting particles (> 50 nm) still grew at that period (Supplement Fig. S4). The coexistence of the shrinkage of new particles and the growth of particles (> 50 nm) has never been reported in the literature. Riipinen et al. (2011) and Ehn et al. (2014) recently reported that SOA condensation was a combination of kinetic condensation and thermodynamically partitioning of vapors on aerosol surface area. Kinetic condensation cannot explain the shrinkage from 21 nm to 17 nm. The possible explanation for the coexistence phenomenon was that the shrinkage of new particles was likely due to the Kelvin effect (Zhang et al., 2012); while particles (> 50 nm) were less affected by the Kelvin effect, and they can grow to CCN size by condensation of species with relatively moderate or high volatility. However, more studies are needed to examine whether the coexistence phenomenon frequently occurs in polluted marine atmosphere and what caused it.

Unlike Day 3, 4 and 5, the two-phase growth of new particles was observed on Day 1 and Day 2. The second-phase growth occurred after a period of stagnation which was regarded as a bottleneck. The modeling results on Day 1 and Day 2 showed that SOA was newly formed and the temporal variation pattern of SOA was consistent with that of the two-phase growth curves of new particles, suggesting the contribution of SOA to the growth of new particles. However, a significant amount of NH_4NO_3 was also formed during two phase growth periods which was different from that on Day 3, 4 and 5. Furthermore, the temporal trend of the modeled NO_3^- and NH_4^+ in mass concentration generally fit the two-phase growth curve. The formation of NH_4NO_3 on Day 1 and Day 2 might be one factor to break up the growth bottleneck, which led to the second-phase growth. In reverse, no newly formed NH_4NO_3 on Day 3, 4 and 5 could be the reason for new particles being unable to break up the growth limit of 30–40 nm.

The modeling results showed that formation of NH_4NO_3 indeed occurred in $PM_{0.1}$ (Supplement Fig. S5a and b) and $PM_{2.5}$ (Figs. 2c and 3c) on Day 1 and Day 2. However, we cannot confirm whether NH_4NO_3 was formed on 30–40 nm particles due to the limitation of CMAQ.

5 Conclusions

Eight NPF events were observed on 5 days out of 31 sampling days during two cruise campaigns in the marginal seas of China. By combining the observational data and the CMAQ modeling results, we inferred that three events were probably caused by photochemical reactions of air pollutants being transported from the continent. However, the causes for other events remain unknown.

Two types of new particles growth patterns were found in the five events, i.e., one-phase growth (18, 19, 26 October 2011) and two-phase growth (4 November 2012, 17 October 2011). The maximum diameters of new particles were in the range of 20–40 nm during the three one-phase growth events and the first-phase growth period in the two-phase growth events. In two-phase growth events, new particles grew from $\sim$ 40 nm to $\sim$ 50 nm in later afternoon or nighttime.

The modeling results suggested that SOA could be an important contributor to the growth of new particles in the one-phase growth events, when no NH_4NO_3 was formed and H_2SO_4 had a negligible contribution to the growth of > 10 nm particles. Formation of NH_4NO_3 and SOA possibly contributed to the growth of new particles in the two-phase growth events. However, the data are still limited and there are unavoidable uncertainties associated with modeling results, especially SOA.

The Supplement related to this article is available online at doi:10.5194/acp-14-7941-2014-supplement.

Acknowledgements. This work is funded by the National Natural Science Foundation of China (41176099, 21190050, 41121004, 41149901), the China Postdoctoral Science Foundation (2012M511548) and the Fundamental Research Funds for the Central Universities (201213008).

Edited by: M. Kulmala

References

Ahlm, L., Liu S., Day, D. A., Russell, L. M., Weber, R., Gentner, D. R., Goldstein, A. H., DiGangi, J. P., Henry, S. B., Keutsch, F. N., VandenBoer, T. C., Markovic, M. Z., Murphy, J. G., Ren, X. R., and Scheller, S.: Formation and growth of ultrafine particles from secondary sources in Bakersfield, California, J. Geophys. Res., 117, D00V08, doi:10.1029/2011jd017144, 2012.

Byun, D. and Ching, J.: Science Algorithms of the EPA Models-3 Community Multiscale Air Quality (CMAQ) Modeling System, EPA Report 600/R-99/030, Washington DC, available at: http://www.epa.gov/amad/Research/CMAQ/CMAQdocumentation.html (last access: 15 May 2013), 1999.

Carlton, A. G., Bhave, P. V., Napelenok, S. L., Edney, E. O., Sarwar, G., Pinder, R. W., Pouliot, G. A., and Houyoux, M.: Model representation of secondary organic aerosol in CMAQ v4.7, Environ. Sci. Technol., 24, 8553–8560, 2010.

Chang, R. Y. W., Sjostedt, S. J., Pierce, J. R., Papakyriakou, T. N., Scarratt, M. G., Michaud, S., Levasseur, M., Leaitch, W. R., and Abbatt, J. P. D.: Relating atmospheric and oceanic DMS levels to particle nucleation events in the Canadian Arctic, J. Geophys. Res., 116, D00S03, doi:10.1029/2011JD015926, 2011.

Charlson, R. J., Lovelock, J. E., Andreae, M. O., and Warren, S. G.: Oceanic phytoplankton, atmospheric sulphur, cloud albedo and climate, Nature, 326, 655–661, doi:10.1038/326655a0, 1987.

Chen, J., Zhang, X. H., and Quan, W. T.: Retrieval chlorophyll *a* concentration from coastal waters: three-band semi-analytical algorithms comparison and development, Opt. Express, 21, 9024–9042, 2013.

Clarke, A. D., Davis, D., Kapustin, V. N., Eisele, F., Chen, G., Paluch, I., Lenschow, D., Bandy, A. R., Yhornton, D., Moore, K., Mauldin, L., Tanner, D., Litchy, M., Carroll, M. A., Collins, J., and Albercook, G.: Particle nucleation in the tropical boundary layer and its coupling to marine sulfur sources, Science, 282, 89–91, 1998.

Curtius, J.: Nucleation of atmospheric aerosol particles, C. R. Phys., 7, 1027–1045, 2006.

Dal Maso, M., Kulmala, M., Riipinen, I., Wagner, R., Hussein, T., Aalto, P. P., and Lehtinen, K. E. J.: Formation and growth of fresh atmospheric aerosols: eight years of aerosol size distribution data from SMEAR II, Hyytiala, Finland, Boreal Environ. Res., 10, 323–336, 2005.

Dall'Osto, M., Harrison, R. M., Furutani, H., Prather, K. A., Coe, H., and Allan, J. D.: Studies of aerosol at a coastal site using two aerosol mass spectrometry instruments and identification of biogenic particle types, Atmos. Chem. Phys. Discuss., 5, 10799–10838, doi:10.5194/acpd-5-10799-2005, 2005.

Dusek, U., Frank, G. P., Hildebrandt, L., Curtius, J., Schneider, J., Walter., S., Chand, D., Drewnick, F., Hings, S., Jung, D., Borrmann, S., and Andreae, M. O.: Size matters more than chemistry for cloud-nucleating ability of aerosol particles, Science, 312, 1375–1378, doi:10.1126/science.1125261, 2006.

Ehn, M., Vuollekoski, H., Petäjä, T., Kerminen, V.-M., Vana, M., Aalto, P., Leeuw, de G., Ceburnis, D., Dupuy, R., O'Dowd, C. D., and Kulmala, M.: Growth rates during coastal and marine new particle formation in western Ireland, J. Geophys. Res., 115, D18218, doi:10.1029/2010JD014292, 2010.

Ehn, M., Thornton, J. A., Kleist, E., Sipilä, M., Junninen, H., Pullinen, L., Springer, M., Rubach, F., Tillmann, R., Lee, B., Lopez-Hilfiker, F., Andres, S., Acir, I.-H., Rissanen, M., Jokinen, T., Schobesberger, S., Kangasluoma, J., Kontkanen, J., Nieminen, T., Kurtén, T., Nielsen, L. B., Jørgensen, S., Kjaergaard, G. H., Canagaratna, M., Dal Maso, M., Berndt, T., Petäjä, T., Wahner, A., Kerminen, V.-M., Kulmala, M., Worsnop, D. R., Wildt, J., and Mentel, T. F.: A large source of low-volatility secondary organic aerosol, Nature, 506, 476–4479, doi:10.1038/ nature13032, 2014.

Feng, J. L., Guo, Z. G., Zhang, T. R., Yao, X. H., Chan, C. K., and Fang, M.: Source and formation of secondary particulate matter in $PM_{2.5}$ in Asian continental outflow, J. Geophys. Res, 117, D03302, doi:10.1029/2011JD016400, 2012.

Holmes, N. S.: A review of particle formation events and growth in the atmosphere in the various environments and discussion of mechanistic implications, Atmos. Environ., 41, 2183–2201, 2007.

Intergovernmental Panel on Climate Change (IPCC): Climate Change 2007: The Physical Science Basis, edited by: Solomon, S., Dahe, Q., Manning, M., Chen, Z., Marquis, M., Averyt, K. B., Tignor, M., and Miller, H. L.: Cambridge Univ. Press, Cambridge, United Kingdom and New York, NY, USA, 153 pp., 2007.

Kerminen, V.-M., Paramonov, M., Anttila, T., Riipinen, I., Fountoukis, C., Korhonen, H., Asmi, E., Laakso, L., Lihavainen, H., Swietlicki, E., Svenningsson, B., Asmi, A., Pandis, S.N., Kulmala, M., and Petäjä, T.: Cloud condensation nuclei production associated with atmospheric nucleation: a synthesis based on existing literature and new results, Atmos. Chem. Phys., 12, 12037–12059, doi:10.5194/acp-12-12037-2012, 2012.

Kulmala, M. and Kerminen, V.-M.: On the formation and growth of atmospheric nanoparticles, Atmos. Res., 90, 132–150, 2008.

Kulmala, M., Kontkanen, J., Junninen, H., Lehtipalo, K., Manninen, H. E., Nieminen, T., Petäjä, T., Sipilä, M., Schobesberger, S., Rantala, P., Franchin, A., Jokinen, T., Järvinen, E., Äijälä, M., Kangasluoma, J., Hakala, J., Aalto, P. P., Paasonen, P., Mikkilä, J., Vanhanen, J., Aalto, J., Hakola, H., Makkonen, U., Ruuskanen, T., Mauldin III, R. L., Duplissy, J., Vehkamäki, H., Bäck, J., Kortelainen, A., Riipinen, I., Kurtén, T., Johnston, M. V., Smith, J. N., Ehn, M., Mentel, T. F., Lehtinen, K. E. J., Laaksonen, A., Kerminen, V.-M., and Worsnop, D. R.: Direct observations of atmospheric aerosol nucleation, Science, 339, 943–946, 2013.

Lin, P., Hu, M., Wu, Z., Niu, Y., and Zhu, T.: Marine aerosol size distributions in the springtime over China adjacent seas, Atmos. Environ., 41, 6784–6796, 2007.

Liu, X. H., Zhang, Y., Cheng, S. H., Xing, J., Zhang, Q., Streets, D. G., Jang, C., Wang, W. X., and Hao, J. M.: Understanding of regional air pollution over China using CMAQ, part I. performance evaluation and seasonal variation, Atmos. Environ., 44, 3719–3727, 2010a.

Liu, X. H., Zhang, Y., Xing, J., Zhang, Q., Wang, K., Streets, D. G., Jang, C., Wang, W. X., and Hao, J. M.: Understanding of regional air pollution over China using CMAQ, part II. Process analysis and sensitivity of ozone and particulate matter to precursor emissions, Atmos. Environ., 44, 3719–3727, 2010b.

Luo, G. and Yu, F.: Sensitivity of global cloud condensation nuclei concentrations to primary sulfate emission parameterizations, Atmos. Chem. Phys., 11, 1949–1959, doi:10.5194/acp-11-1949-2011, 2011.

O'Dowd, C. D. and Leeuw, de G.: Marine aerosol production: a review of the current knowledge, Philos. T. R. Soc. A, 365, 1753–1774, 2007.

O'Dowd, C. D., Jimenez, J. L., Bahreini, R., Flagan, R. C., Seinfeld, J. H., Pirjola, L., Kulmala, M., Jennings, S. G., and Hoffmann, T.: Marine aerosol formation from biogenic iodine emissions, Nature, 417, 632–636, 2002.

O'Dowd, C. D., Yoon, Y. J., Junkerman, W., Aalto, P., Kulmala, M., Lihavainen, H., and Viisanen, Y.: Airborne measurements of nucleation mode particles I: coastal nucleation and growth rates, Atmos. Chem. Phys., 7, 1491–1501, doi:10.5194/acp-7-1491-2007, 2007.

O'Dowd, C. D., Monahan, C., and Dall'Osto, M.: On the occurrence of open ocean particle production and growth events, Geophys. Res. Lett., 37, L19805, doi:10.1029/2010GL044679, 2010.

Paasonen, P., Nieminen, T., Asmi, E., Manninen, H. E., Petäjä, T., Plass-Dülmer, C., Flentje, H., Birmili, W., Wiedensohler, A., Hõrrak, U., Metzger, A., Hamed, A., Laaksonen, A., Facchini, M. C., Kerminen, V.-M., and Kulmala, M.: On the roles of sulphuric acid and low-volatility organic vapours in the initial steps of atmospheric new particle formation, Atmos. Chem. Phys., 10, 11223–11242, doi:10.5194/acp-10-11223-2010, 2010.

Petters, M. D. and Kreidenweis, S. M.: A single parameter representation of hygroscopic growth and cloud condensation nucleus activity, Atmos. Chem. Phys., 7, 1961–1971, doi:10.5194/acp-7-1961-2007, 2007.

Pierce, J. R. and Adams, P. J.: Can cosmic rays affect cloud condensation nuclei by alterIng new particle formation rates?, J. Geophys. Res., 36, L09820, doi:10.1029/2009GL037946, 2009.

Pierce, J. R., Leaitch, W. R., Liggio, J., Westervelt, D. M., Wainwright, C. D., Abbatt, J. P. D., Ahlm, L., Al-Basheer, W., Cziczo, D. J., Hayden, K. L., Lee, A. K. Y., Li, S.-M., Russell, L. M., Sjostedt, S. J., Strawbridge, K. B., Travis, M., Vlasenko, A., Wentzell, J. J. B., Wiebe, H. A., Wong, J. P. S., and Macdonald, A. M.: Nucleation and condensational growth to CCN sizes during a sustained pristine biogenic SOA event in a forested mountain valley, Atmos. Chem. Phys., 12, 3147–3163, doi:10.5194/acp-12-3147-2012, 2012.

Quinn, P. K. and Bates, T. S.: The case against climate regulation via oceanic phytoplankton sulphur emissions, Nature, 480, 51–56, 2011.

Quinn, P. K., Bates, T. S., Coffman, D. J., and Covert, D. S.: Influence of particle size and chemistry on the cloud nucleating properties of aerosols, Atmos. Chem. Phys., 8, 1029–1042, doi:10.5194/acp-8-1029-2008, 2008.

Riipinen, I., Pierce, J. R., Yli-Juuti, T., Nieminen, T., Häkkinen, S., Ehn, M., Junninen, H., Lehtipalo, K., Petäjä, T., Slowik, J., Chang, R., Shantz, N. C., Abbatt, J., Leaitch, W. R., Kerminen, V.-M., Worsnop, D. R., Pandis, S. N., Donahue, N. M., and Kulmala, M.: Organic condensation: a vital link connecting aerosol formation to cloud condensation nuclei (CCN) concentrations, Atmos. Chem. Phys., 11, 3865–3878, doi:10.5194/acp-11-3865-2011, 2011.

Riipinen, I., Yli-Juuti, T., Pierce, J. R., Petäjä, T., Worsnop, D. R., Kulmala, M., and Donahue, N. M.: The contribution of organics to atmospheric nanoparticle growth, Nat. Geosci., 5, 453–458, doi:10.1038/NGEO1499, 2012.

Shi, J. H., Gao, H. W., Qi, J. H., Zhang, J., and Yao, X. H.: Sources, compositions, and distributions of water-soluble organic nitrogen in aerosols over the China Sea, J. Geophys. Res: Atmos, 115, D17303, doi:10.1029/2009JD013238, 2010.

Skamarock, W. C., Klemp, J. B., Dudhia, J., Gill, D. O., Barker, D. M., Duda, M., Huang, X. Y., Wang, W., and Powers, J. G.: A description of the advanced research WRF version 3, NCAR, Tech. Note, Mesoscale and Microscale Meteorology Division, National Center for Atmospheric Research, Boulder, Colorado, USA, 2008.

Sloane, C. S., Rood, M. J., and Rogers, C. F.: Measurements of aerosol particle size-improved precision by simultaneous use of optical particle counter and nephelometer, Aerosol Sci. Tech., 14, 289–301, 1991.

Smith, S. N. and Mueller, S. F.: Modeling natural emissions in the Community Multiscale Air Quality (CMAQ) Model–I: building an emissions data base, Atmos. Chem. Phys., 10, 4931–4952, doi:10.5194/acp-10-4931-2010, 2010.

Smith, J. N., Dumn, M. J., VanReken, T. M., Iida, K., Stolzenburg, M. R., McMurry, P. H., and Huey, L. G.: Chemical composition of atmospheric nanoparticles formed from nucleation in Tecamac, Mexico: evidence for an important role for organic species in nanoparticles growth, J. Geophys. Res., 35, L04808, doi:10.1029/2007GL032523, 2008.

Tan, S. C., Shi, G. Y., Shi, J. H., Gao, H. W., and Yao, X. H.: Correlation of Asian dust with chlorophyll and primary productivity in the coastal seas of China during the period from 1998 to 2008, J. Geophys. Res., 116, G02029, doi:10.1029/2010JG001456, 2011.

Wang, Y., Zhang, R. Y., and Saravanan, R.: Asian pollution climatically modulates mid-latitude cyclones following hierarchical modelling and observational analysis, Nat. Commun., 5, doi:10.1038/ncomms4098, 2014.

Whitby, K. T.: The physical characteristics of sulphur aerosols, Atmos. Environ., 12, 135–159, 1978.

Yang, G. P., Zhang, H. H., Su, L. P., and Zhou, L. M.: Biogenic emission of dimethylsulfide (DMS) from the North Yellow Sea, China and its contribution to sulfate in aerosol during summer, Atmos. Environ., 43, 2196–2203, 2009.

Yao, X. H. and Zhang, L.: Sulfate formation in atmospheric ultrafine particles at Canadian inland and coastal rural environments, J. Geophys. Res, 116, D10202, doi:10.1029/2010JD015315, 2011.

Yao, X. H., Lau, N. T., Fang, M., and Chan, C. K.: Real-time observation of the transformation of ultrafine atmospheric particle modes, Aerosol Sci. Tech., 39, 831–841, 2005.

Yao, X. H., Chio, M. Y., Lau, N. T., Lau, A. P. S., Chan, C. K., and Fang, M.: Growth and shrinkage of new particles in the atmosphere in Hong Kong, Aerosol Sci. Tech., 44, 639–650, 2010.

Young, L.-H., Lee, S.-H., Kanawade, V. P., Hsiao, T.-C., Lee, Y. L., Hwang, B.-F., Liou, Y.-J., Hsu, H.-T., and Tsai, P.-J.: New particle growth and shrinkage observed in subtropical environments, Atmos. Chem. Phys., 13, 547–564, doi:10.5194/acp-13-547-2013, 2013.

Zhang, Q., Streets, D. G., Carmichael, G. R., He, K. B., Huo, H., Kannari, A., Klimont, Z., Park, I. S., Reddy, S., Fu, J. S., Chen, D., Duan, L., Lei, Y., Wang, L. T., and Yao, Z. L.: Asian emissions in 2006 for the NASA INTEX-B mission, Atmos. Chem. Phys., 9, 5131–5153, doi:10.5194/acp-9-5131-2009, 2009.

Zhang, R., Wang, L., Khalizov, A. F., Zhao, J., Zheng, J., McGraw, R. L., and Molina, L. T.: Formation of nanoparticles of blue haze enhanced by anthropogenic pollution, PANS, 106, 17650–17654, 2009.

Zhang, R., Khalizov, A., Wang, L., Hu, M., and Xu, W.: Nucleation and growth of nanoparticles in the atmosphere, Chem. Rev., 112, 1957–2011, 2012.